2016 American Control Conference (ACC)
Boston Marriott Copley Place
July 6-8, 2016. Boston, MA, USA

Design of a Higher Order Attachment for the Quanser Qube

Diane L. Peters, *Senior Member, IEEE*

Abstract— **In the development of lab exercises for a Dynamic Systems with Controls lab, one constraint on the chosen hardware was that certain types of labs could not be performed. The hardware that was being used, the Quanser Qube, had two existing attachments; with one attachment, an inertial disc, the system was fundamentally a first-order plant. The second attachment, an inverted pendulum, was non-linear and unstable. Neither attachment provided an example of a second-order underdamped plant, nor could a lab be performed with Ziegler-Nichols PID tuning. In order to address these issues, new attachments could be designed and constructed for the Qube, which would add to its range of possible lab exercises. In this paper, one new attachment is described. This attachment features two inertias with compliance and damping. It was designed based on a theoretical model, in order to have certain desired dynamic characteristics, and then model validation was performed. It was found that there were significant unmodeled effects, and an empirical model was derived for the attachment. Due to these effects, the attachment was also limited, and a Ziegler-Nichols lab was still not possible. However, it was possible to perform other lab exercises using this attachment. Based on the empirical model, a sample lab exercise was designed, and an appropriate LabVIEW VI was constructed.**

I. Introduction

In controls classes, it is well established that students need to have a good understanding of the practical applications of control, not only the theoretical basis for it. In the Controls Curriculum Survey conducted by the IEEE Control Systems Society in 2009, industry practitioners were quoted as follows: "Controls curricula focus too much on math and not enough on physical intuition", and "Control engineers need to be more holistic. Need to understand the physics of the application in at least some domains, be able to develop first principles based models and also be able to connect on the implementation level (real time, embedded implementation). The current curriculum emphasized the mathematical theory at the expense of the practical realization aspects." [1] Effective laboratory experiences help students to learn the implementation of what they learn, giving them skills desired by industry. In order to provide such an effective laboratory experience, labs need to be equipped with appropriate hardware. There are many choices available for laboratory hardware, and the decision on what is the most appropriate choice is an important issue for many universities as they develop and implement lab experiences for their students, as discussed in [2, 3], and many ideas have been put forth and tried at different institutions [4, 5, 6]. Laboratory equipment can be designed from the ground up [7, 8], purchased from a manufacturer, or some combination.

D. L. Peters is with Kettering University, Flint, MI 48504 USA (phone: 810-762-7916; fax: 810-762-7860; e-mail: dpeters@kettering.edu).

At Kettering University, the Quanser Qube was chosen for inclusion in the Dynamic Systems with Controls laboratory, due to its cost, ability to be integrated with LabVIEW, and the availability of pre-designed labs from the manufacturer. The Qube has been integrated into the laboratory, as described in [9]; however, there are some labs that cannot be performed with this equipment, and therefore a new attachment has been designed for the Qube. The development of this attachment, its dynamic characteristics, and its potential use in desired labs are the subjects of this paper.

II. Description of the Quanser Qube

A. Basic Configuration of the Qube

The Quanser Qube consists of a black cube, approximately 4 inches in size, which contains a DC motor. The Qube has a hub on the top, on which two available attachments can be fastened using magnets. One of these attachments is a simple inertial disk, and the other is an inverted pendulum. The Qube can be controlled using the National Instruments myRIO controller, which is programmed using LabVIEW. The basic setup for the Qube is shown in Fig. 1.

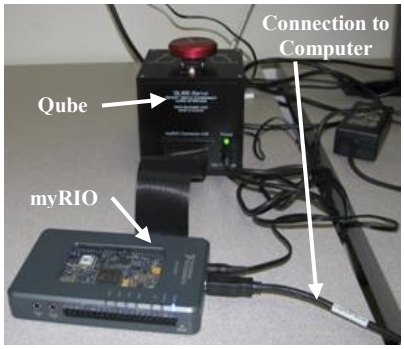

Figure 1: Basic Setup of Qube and myRIO

A variety of labs can be conducted using the Qube; Quanser provides appropriate files (lab documentation and appropriate LabVIEW Virtual Instruments) for 9 labs using the inertial disk (7 fundamental labs and 2 application labs), and 6 labs using the inverted pendulum [10]. However, while there are many available labs, there are some labs that cannot be conducted with either of these attachments. For example, with the inertial disc the plant may be modeled either as a first-order system or as a heavily overdamped second-order system, with one dominant pole and one extremely fast pole that produces no noticeable effect on the system. In order to exhibit second-order behavior, a controller needs to be used. The system is unsuitable for a Ziegler-Nichols Process Reaction Method (PRM) lab, since this requires either a higher order system or a time delay. This system also cannot be used for a Ziegler-Nichols Ultimate Cycle Method (UCM)

tuning lab, as described in the next section. In order to perform such a lab exercise, it is necessary to have a system which is initially stable, but which can be made marginally stable by applying a sufficiently high proportional gain. The inverted pendulum, of course, is both unstable and non-linear, and therefore not suitable for such a lab.

B. Dynamic Characteristics of the Quanser Qube with Inertial Disk

A DC motor can be modeled as a second-order system, with its transfer function for the velocity relative to input voltage given by the relation

$$G(s) = \frac{k_m}{J_{eq}L_m s^2 + R_m J_{eq} s + k_m^2} \tag{1}$$

where the symbols are defined in Table 1. If the inductance is sufficiently low, however, a first-order model can be used to represent the system, with the transfer function for the velocity relative to input voltage given by the relation

$$G(s) = \frac{k_m}{R_m J_{eq} s + k_m^2} \tag{2}$$

This is the case for the Qube, as documented in the technical information and lab files provided by Quanser [8]; values of the relevant parameters for the Qube, as supplied by Quanser, are given in Table 1.

TABLE I. DEFINITIONS AND VALUES OF PARAMETERS FOR QUBE [8]

Parameter	Definition	Value	Units
k_m	Motor constant	0.036	N-m/A
R_m	Armature resistance of motor	6.3	Ω
L_m	Armature inductance of motor	0.85	mH
J_{eq}	Equivalent inertia; sum of rotor inertia of the motor, hub inertia, and inertia of the disk	2.168×10^{-5}	kg-m^2

In this case, the transfer function for the angular position of the disk is second order, with one pole at zero and one negative real pole. As previously stated, this system cannot be used for the study of second-order underdamped systems without a controller; nor can it be used for a Ziegler-Nichols lab. It exhibits neither a time delay nor higher order behavior, which are required for the PRM method, and application of a proportional gain simply cannot result in a marginally stable system, which is required for UCM.

Even if a second-order model is retained for the velocity, resulting in a third-order model for the angular position of the disk, the system will not be underdamped, will not exhibit the proper behavior for the PRM method, and also cannot achieve marginal stability with any realistic value of the proportional gain. Using the higher-order model with the $j\omega$ method of calculating the ultimate gain and ultimate period yields the following expressions:

$$K_u = \frac{R_m k_m}{L_m} \tag{3}$$

$$P_u = \frac{2\pi\sqrt{J_{eq}L_m}}{k_m} \tag{4}$$

For the values given in Table 1, this means the ultimate gain K_u = 266.8, the ultimate period P_u = 23.7 ms, and the maximum voltage required by the controller is over 250 V for a unit step input; clearly, this is an unrealistic scenario.

III. DESIGN OF THE ATTACHMENT

A. Basic Configuration of the Attachment

The attachment that was designed and constructed for the Qube, utilizing its existing method of attachment with magnets, is shown in Fig. 2. This attachment features two inertias, one of which is directly coupled to the Qube's DC motor. Between the two inertias, there is a torsional spring (item 6) providing compliance, and a certain amount of damping inherent in the ball bearing (item 2). A hollow-shaft encoder (item 7) is mounted on the second inertia and coupled to the first, providing feedback on the relative angular positions of the two inertias. Together with the encoder in the Qube's housing which measures the DC motor's rotation, it is possible to obtain position feedback for both inertias, and therefore to measure the velocity of each inertia as well.

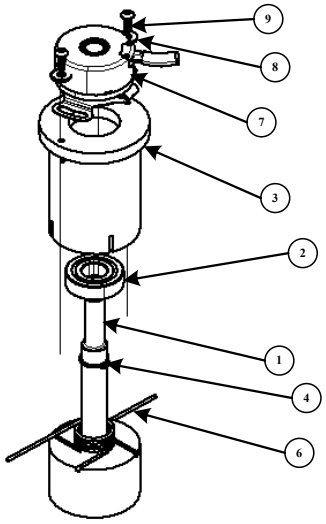

Figure 2: Design of Attachment for Quanser Qube

B. Dynamic Characteristics of the Quanser Qube with Attachment

A dynamic model of the attachment mounted on the Qube was constructed, using the bond graph approach, as shown in Fig. 3. Due to the low inductance of the DC motor in the Qube, it was omitted from the model, leaving three independent energy storage elements – the two inertias as well as the spring.

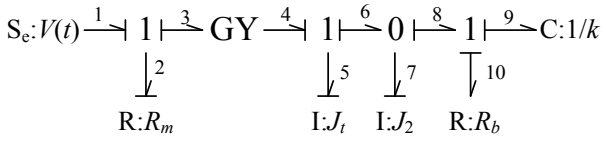

Figure 3: Bond Graph Model of Qube Attachment

$$\begin{bmatrix}\dot{p}_5\\ \dot{p}_7\\ \dot{q}_9\end{bmatrix}=\begin{bmatrix}-\dfrac{k_m^2+R_mR_b}{J_tR_m} & \dfrac{R_b}{J_2} & -k\\ \dfrac{R_b}{J_t} & -\dfrac{R_b}{J_2} & k\\ \dfrac{1}{J_t} & -\dfrac{1}{J_2} & 0\end{bmatrix}\begin{bmatrix}p_5\\ p_7\\ q_9\end{bmatrix}+\begin{bmatrix}\dfrac{k_m}{R_m}\\ 0\\ 0\end{bmatrix}V(t) \quad (5)$$

$$\begin{bmatrix}\omega_1\\ \omega_2\\ \Delta\theta\\ i\end{bmatrix}=\begin{bmatrix}\dfrac{1}{J_t} & 0 & 0\\ 0 & \dfrac{1}{J_2} & 0\\ 0 & 0 & 1\\ -\dfrac{k_m}{R_mJ_t} & 0 & 0\end{bmatrix}\begin{bmatrix}p_5\\ p_7\\ q_9\end{bmatrix}+\begin{bmatrix}0\\ 0\\ 0\\ \dfrac{1}{R_m}\end{bmatrix}V(t) \quad (6)$$

Using this bond graph, the state equation for the system was derived. Four outputs were selected for this system: the angular velocity of each inertia, the angular position of the second inertia (item 3) with respect to the first, and the current in the system. This yields Eq. (5) and (6),.where the parameters of the attachment are described, and values given where available, in Table 2. The values of each inertia can be calculated from the solid model of the attachment, as well as the data provided by Quanser for the Qube. The spring constant is a manufacturer-provided parameter. However, the bearing resistance is unknown, since the requisite information is not readily available from the manufacturer, and would need to be determined experimentally.

TABLE II. DEFINITIONS AND VALUES OF PARAMETERS FOR ATTACHMENT

Parameter	Definition	Value	Units
R_b	Bearing resistance	UNKNOWN	N-m-s/rad
J_t	Total inertia coupled directly to the motor; sum of rotor inertia of the motor, hub inertia, and inertia of item 1 in the attachment	$9.088\text{x}10^{-5}$	kg-m^2
k	Spring constant for the torsional spring	0.198	N-m/rad
J_2	Inertia that occurs after the spring; sum of the inertia of item 3 in the attachment and of the encoder	$7.995\text{x}10^{-5}$	kg-m^2

Note that, although the absolute positions of the inertias cannot be expressed in terms of states and the input $V(t)$, the transfer functions for them can be readily obtained from the transfer functions for the angular velocities by integration. The full set of transfer functions for the original four outputs, plus the angular positions of the inertias, is given by Eq. (7) – (12).

$$G_1(s)=\frac{\Omega_1(s)}{V(s)}=\frac{k_m\left(J_2s^2+R_bs+k\right)}{R_mJ_2J_ts^3+\left(k_m^{\,2}J_2+R_bJ_2R_m+R_bJ_tR_m\right)s^2+\left(R_bk_m^{\,2}+kJ_tR_m+kJ_2R_m\right)s+kk_m^{\,2}} \quad (7)$$

$$G_2(s)=\frac{\Omega_2(s)}{V(s)}=\frac{k_m\left(R_bs+k\right)}{R_mJ_2J_ts^3+\left(k_m^{\,2}J_2+R_bJ_2R_m+R_bJ_tR_m\right)s^2+\left(R_bk_m^{\,2}+kJ_tR_m+kJ_2R_m\right)s+kk_m^{\,2}} \quad (8)$$

$$G_3(s)=\frac{\Delta\Theta(s)}{V(s)}=\frac{k_mJ_2s}{R_mJ_2J_ts^3+\left(k_m^{\,2}J_2+R_bJ_2R_m+R_bJ_tR_m\right)s^2+\left(R_bk_m^{\,2}+kJ_tR_m+kJ_2R_m\right)s+kk_m^{\,2}} \quad (9)$$

$$G_4(s)=\frac{I(s)}{V(s)}=\frac{J_2J_ts^3+R_b\left(J_2+J_t\right)s^2+k\left(J_2+J_t\right)s}{R_mJ_2J_ts^3+\left(k_m^{\,2}J_2+R_bJ_2R_m+R_bJ_tR_m\right)s^2+\left(R_bk_m^{\,2}+kJ_tR_m+kJ_2R_m\right)s+kk_m^{\,2}} \quad (10)$$

$$G_5(s)=\frac{\Theta_1(s)}{V(s)}=\frac{k_m\left(J_2s^2+R_bs+k\right)}{R_mJ_2J_ts^4+\left(k_m^{\,2}J_2+R_bJ_2R_m+R_bJ_tR_m\right)s^3+\left(R_bk_m^{\,2}+kJ_tR_m+kJ_2R_m\right)s^2+kk_m^{\,2}s} \quad (11)$$

$$G_6(s)=\frac{\Theta_2(s)}{V(s)}=\frac{k_m\left(R_bs+k\right)}{R_mJ_2J_ts^4+\left(k_m^{\,2}J_2+R_bJ_2R_m+R_bJ_tR_m\right)s^3+\left(R_bk_m^{\,2}+kJ_tR_m+kJ_2R_m\right)s^2+kk_m^{\,2}s} \quad (12)$$

C. Model Validation and Empiricallly Derived Model

Model validation proved to be somewhat difficult in practice, in large part because of unmodeled effects. As shown in Fig. 4, the system had an encoder cable which provided a certain degree of resistance. This resistance changed, based on the position of the cable when the test was being run. Other unmodeled effects could include the resistance in the bearing, which was assumed to be linear; this assumption was not verified, however, and appropriate bearing resistance information is not available from typical manufacturers' catalogs. Therefore, while the system design was based on the theoretical dynamic model, lab development was based on an empirically derived model.

In order to derive this model, a series of tests was conducted, including both step inputs and sinusoidal inputs. For the sinusoidal inputs, different frequencies were used and the gain was tabulated for these frequencies. Due to the

unpredictable effects of the encoder cable, there was a considerable amount of error in some of the results.

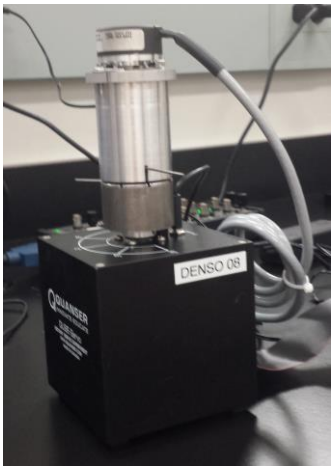

Figure 4: Qube Attachment

A magnitude plot was constructed for the output of the encoder giving the position of Inertia 1, as shown in Fig. 5. The step response of the attachment was also analyzed, with the results shown in Fig. 6. A transfer function was derived empirically, as given by Eq. (13), and compared to both the frequency data and the step data; these comparisons are also shown in Fig. 5 & 6.

$$G(s)=\frac{10.368(0.075s+1)(s^2+20s+100)}{(0.025s+1)(s^2+6s+36)(s^2+13.2s+144)} \quad (13)$$

There is a significant amount of scatter in the data, and at the lower frequencies in particular it is not obvious that the magnitude plot is correct. However, the step plot is much clearer, and gives a better idea of what the behavior is like at those low frequencies.

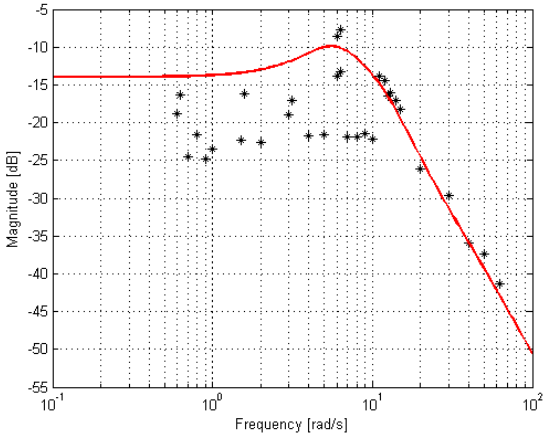

Figure 5: Frequency Response of Attachment

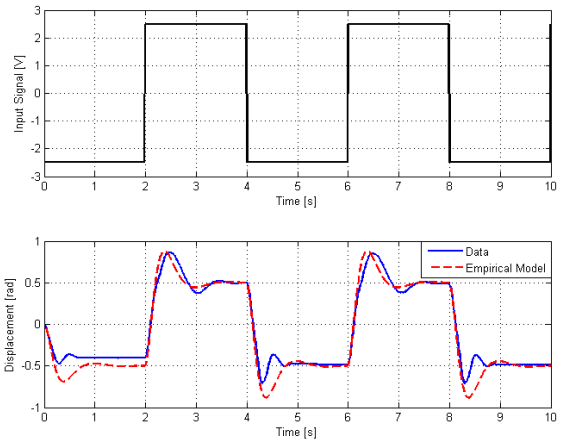

Figure 6: Step Response of Attachment

D. *Analysis of Empirical Model*

This particular empirical model matches the steady-state value well, and shows a good match to the dynamics of the system when it is displaced in the positive direction. In the negative direction, its overshoot is more than is actually seen in the data, most likely due to the effects of the encoder cable pulling on the system. The full Bode plot of Eq. (13), including the phase plot, as well as its response to a unit step, are given in Fig. 7 & 8, respectively.

While the step response does look very similar to that of a simple second-order system, a careful look at its characteristics close to the beginning of the plot does look slightly different; as it is in fact a higher order model, there is an upward curve. In theory, this would allow the attachment to be used for a lab in which the Ziegler-Nichols Process Reaction Method (PRM) is used, since this this method relies upon a time delay in the system. However, the time delay found by fitting a straight line tangent to the step response would be very small, and in practice such a lab is most likely not feasible due to uncertainties in the measured data. However, it does suggest that an attachment of this type, with different parameters, could be used for such a lab.

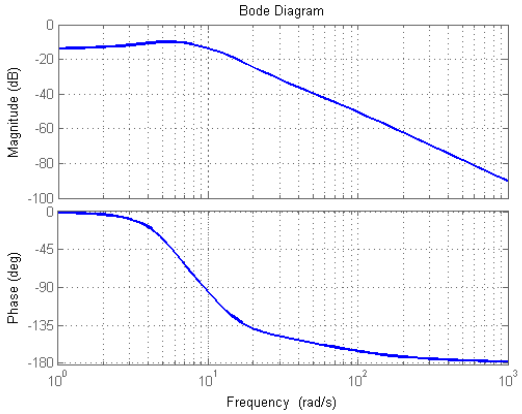

Figure 7: Bode Plot of Empirical Model

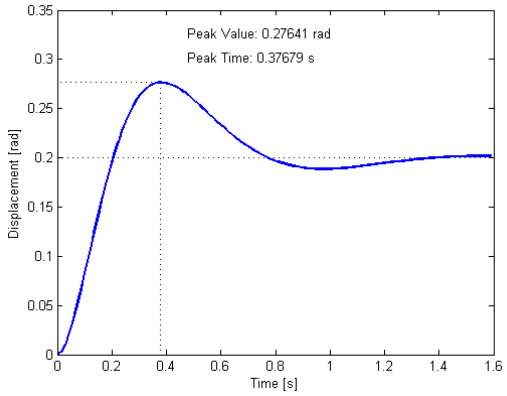

Figure 8: Step Response of Empirical Model

Given the empirically derived model of the attachment, a root locus plot was constructed for the transfer function for Inertia 1, as shown in Fig. 9. It can be seen that, while the attachment has a far more complex root locus plot than a simple first-order or second-order overdamped system, e.g., the inertial disc, the system cannot be made marginally stable. Therefore, while a number of interesting labs can be done with the attachment, it still is limited in that a Ziegler-Nichols PID lab cannot be performed with it. It is believed that this difference between the original design goal of the attachment and the actual performance of the empirical model is due to the higher than anticipated amount of damping, both from the bearing and from the encoder cable. While increases in the mass of the attachment would change the system dynamics, it is necessary to be cautious about this to avoid having so much inertia that the magnets cannot keep the attachment in place during operation.

IV. Development of Lab Exercises

After the attachment itself was developed and its characteristics were analyzed, a lab exercise was designed in which students would be able to look at its step response and frequency response. The purpose of the lab exercise would be to introduce the students to the concept of model validation, and show how they could compare a theoretical model to experimental data.

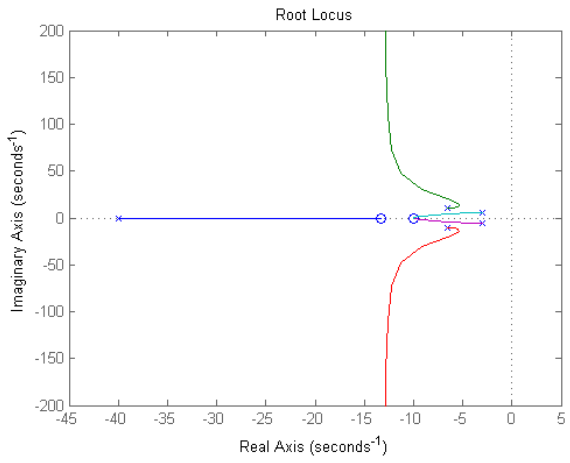

Figure 9: Root Locus Plot for Attachment

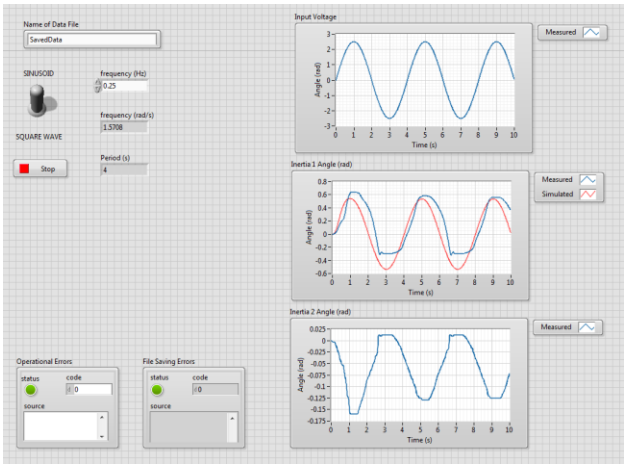

Figure 10: Front Panel of VI for Sample Lab

The interface for the system was constructed using the National Instruments software LabVIEW, with the front panel of the Virtual Instrument (VI) shown in Fig. 10. Students would be able to choose either a sine wave or a square wave, and would be able to specify the frequency in Hz. The display would give both the frequency in rad/s, the period of the signal, and graphs of signals. It also allows students to specify a filename; by doing so, the time, voltage, and encoder data would be saved to a *.csv file on a flash drive plugged into the myRIO controller. The VI also includes error handling, so that the student will be alerted if the file fails to save properly (e.g., if he or she has forgotten to plug the flash drive into the myRIO), or if the there is an error in the operation of the hardware, such as the motor in the Qube stalling.

The interface shows the theoretical model and the actual signal from Inertia 1; it also shows the signal from the second encoder, without any model data. Students can then, in a simple lab, evaluate the match between the empirically derived model given here and the experimental data. The block diagram for the VI, including the transfer function for the system as well as all the data processing, is shown in Fig. 11. The VI is currently configured to run for 10 seconds, although this could be modified to a user-defined value. Furthermore, the VI can be stopped at any time by the user, by means of the "STOP" button on the front panel.

In future, the VI could also be modified to allow for more than two choices of input functions. The input signal is not intrinsically limited to the sine wave or step, although for the sake of simplicity only those two choices are provided to the student in this lab exercise (via the toggle switch on the front panel). Other signals, such as a sawtooth or a random signal, could be allowed if desired.

If a more complex lab experience was desired, then students could derive a model for the data from the second encoder. In order to do that, the data that was saved to the flash drive could be manipulated in MS Excel or Matlab to extract gains and step response characteristics, and to compare to a possible model.

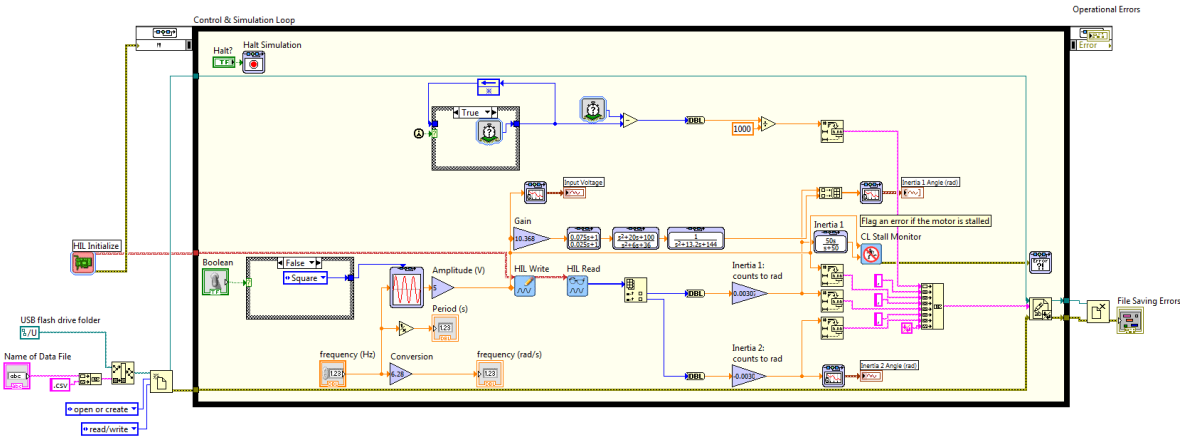

Figure 11: Block Diagram for Sample Lab

V. Conclusion

This paper describes the development of a new attachment for the Quanser Qube. The attachment was developed based on a theoretical dynamic model; however, as a result of significant unmodeled effects, the dynamic model used for development did not adequately describe the performance of the attachment. Therefore, an empirical model was derived from the data, and this model was used for the development of a possible lab using the attachment.

The attachment can still be improved significantly. For example, it may be possible to reduce the effects of the encoder cable on the system. By shortening the cable, its weight will be decreased, and there will be less loose cable to interfere with the motion. However, the length of the cable cannot be too short, in order to provide for a sufficient range of motion for the attachment's rotation. Other improvements could include finding a bearing with less friction, in order to provide more oscillation in the response. In addition, if a less stiff spring could be used, it would be possible to remove mass and make the entire device more compact, and it is hoped that some of these changes would allow the attachment to have the desired characteristics for activities such as a Ziegler-Nichols UCM PID tuning lab.

Other types of attachments could be devised to expand the range of activities that could be performed with the Qube. Such attachments could include simple machines to be controlled, such as linkages, gears, or belt drives, as well as interesting devices such as a ball governor. The ball governor, in particular, would demonstrate to students what types of mechanical control devices were once used, by showing the relationship between angular speed and the position of the balls. It is expected that many other attachments, both those designed by faculty teaching labs and by students using the equipment, could be designed and used in a variety of ways. The nature of these attachments is also a subject of future work, and it is hoped that such attachments will be developed and shared with the community using the Qube.

Acknowledgment

Thanks to Quanser for supplying the necessary magnets and the encoder cable and necessary interface information for the construction of this attachment.

References

[1] Cook, J.A. & T. Sama. "Controls Curriculum Survey: A CSS Outreach Task Force Report." IEEE Control Systems Society, 2009.

[2] Franklin, G. F. & J. D. Powell. "Digital Control Laboratory Courses." Control Systems Magazine, IEEE, 9(3), 1989.

[3] Thompson, J. G., P. J. Gorder, & W. N. White. "Integration of Flexible Embedded Control System Design into the Mechanical Engineering Curriculum." in Proceedings of the American Control Conference, Seattle, WA, June 1995.

[4] Gunasekaran, M. & R. Potluri. "Low-Cost Undergraduate Control Systems Experiments using Microcontroller-Based Control of a DC Motor." IEEE Transactions on Education, 2012, 55(4), pp. 508-516.

[5] Peerless, K. T., J. M. Panosian, & P. A. Hassanpour. "Design and Implementation of a General Control System Platform." in *Proceedings of the ASME International Mechanical Engineering Congress and Exposition*, Montreal, Canada, 2014.

[6] Vasquez, R. E., N. L. Posada, F. Castrillon, & D. Giraldo. "Development of a Laboratory Equipment for Dynamic Systems and Process Control Education." in *Proceedings of the ASME International Mechanical Engineering Congress and Exposition*, Montreal, Canada, 2014.

[7] Reck, R. M. & R. S. Sreenivas. "Developing an Affordable Laboratory Kit for Undergraduate Controls Education." in *Proceedings of the ASME Dynamic Systems and Controls Conference*, San Antonio, TX, 2014.

[8] Reck, R. M. & R. S. Sreenivas. "Developing a New Affordable DC Motor Laboratory Kit for an Existing Undergraduate Controls Course." in *Proceedings of the American Control Conference*, Chicago, IL, 2015.

[9] Peters, D. L., R. Stanley, C. Hoff, and J. Casci "Redesign of lab experiences for a senior level course in dynamic systems with controls," in *Proceedings of the ASEE Annual Conference*, Seattle, WA, June 2015.

[10] Quanser Courseware website, http://www.quanser.com/courseware/qubeservo_labview/, accessed on 9/18/2015